Aeroelastic Instabilities of Large Offshore and Onshore Wind Turbines

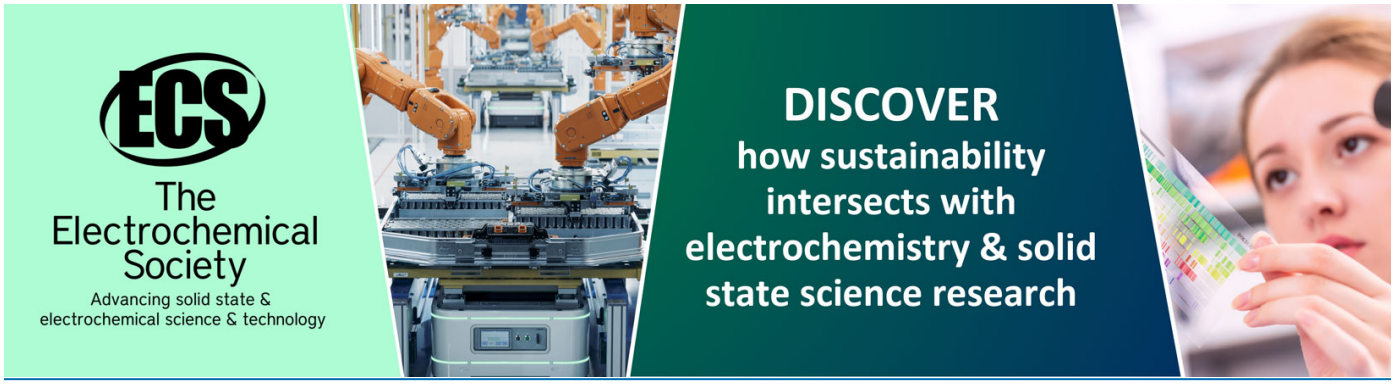

Journal of Physics: Conference Series **75** (2007) 012069 doi:10.1088/1742-6596/75/1/012069

Aeroelastic Instabilities of Large Offshore and Onshore Wind Turbines

Gunjit Bir and Jason Jonkman

National Renewable Energy Laboratory
1617 Cole Blvd, Golden, CO 80401, USA

E-mail: Gunjit_bir@nrel.gov

Abstract. Offshore turbines are gaining attention as means to capture the immense and relatively calm wind resources available over deep waters. This paper examines the aeroelastic stability of a three-bladed 5MW conceptual wind turbine mounted atop a floating barge with catenary moorings. The barge platform was chosen from the possible floating platform concepts, because it is simple in design and easy to deploy. Aeroelastic instabilities are distinct from resonances and vibrations and are potentially more destructive. Future turbine designs will likely be stability-driven in contrast to the current loads-driven designs. Reasons include more flexible designs, especially the torsionally-flexible rotor blades, material and geometric couplings associated with smart structures, and hydrodynamic interactions brought on by the ocean currents and surface waves. Following a brief description of the stability concept and stability analysis approach, this paper presents results for both onshore and offshore configurations over a range of operating conditions. Results show that, unless special attention is paid, parked (idling) conditions can lead to instabilities involving side-to-side motion of the tower, edgewise motion of the rotor blades, and yawing of the platform.

1. Introduction

Offshore turbines have the potential to capture the immense wind resources available over sea waters. Diverse concepts have been proposed for shallow, deep, and intermediate-depth waters. References 1-4 provide an overview of the energy resources at these depths and the associated technologies. In the United States, China, Japan, Norway, and several other countries, deep water offers the most potential for offshore wind resource capture. Floating platforms, with wind turbines mounted atop, appear to be the most economical for these depths [2,4]. Of the several configurations possible for floating platforms, Figure 1 shows three configurations that appear promising. They differ in their mechanisms to attain static stability. The spar-buoy configuration uses ballast to lower the center-of-gravity below the center-of-buoyancy and is moored either by catenaries (shown) or by taut lines. The tension leg platform (TLP) uses mooring lines, which stay in tension due to the excess buoyancy provided by the hollow platform (tank). The barge configuration achieves stability through waterline buoyancy of the barge and is moored by catenaries. References 5-12 discuss modeling and engineering issues associated with these configurations.

This paper examines the aeroelastic stability characteristics of a barge platform over a range of operating conditions. We selected the barge platform because it offers design simplicity, cost-effective construction, and easy installation. Aeroelastic instabilities, as discussed in the next section, are distinct from resonances and vibrations and are potentially more destructive. Future turbine designs

will likely be stability-driven in contrast to the current loads-driven designs. These designs will very likely use advanced features such as tailored composites, torsionally-flexible curved blades, smart structures, and fast-acting controls to mitigate loads, enhance performance, and reduce cost. These features may lead to instabilities because of the yet-unknown aero-servo-elastic-type dynamic interactions. Examples of known instabilities, for structures with fixed or rotary wings, are blade pitch-flap flutter [13-17], stall-induced vibration [18-23], rotor-shaft whirl [24,25], and aeromechanical instability [13,26,27]. Offshore turbines might be more susceptible to instabilities because of the additional hydrodynamic interactions brought on by the ocean currents and surface waves.

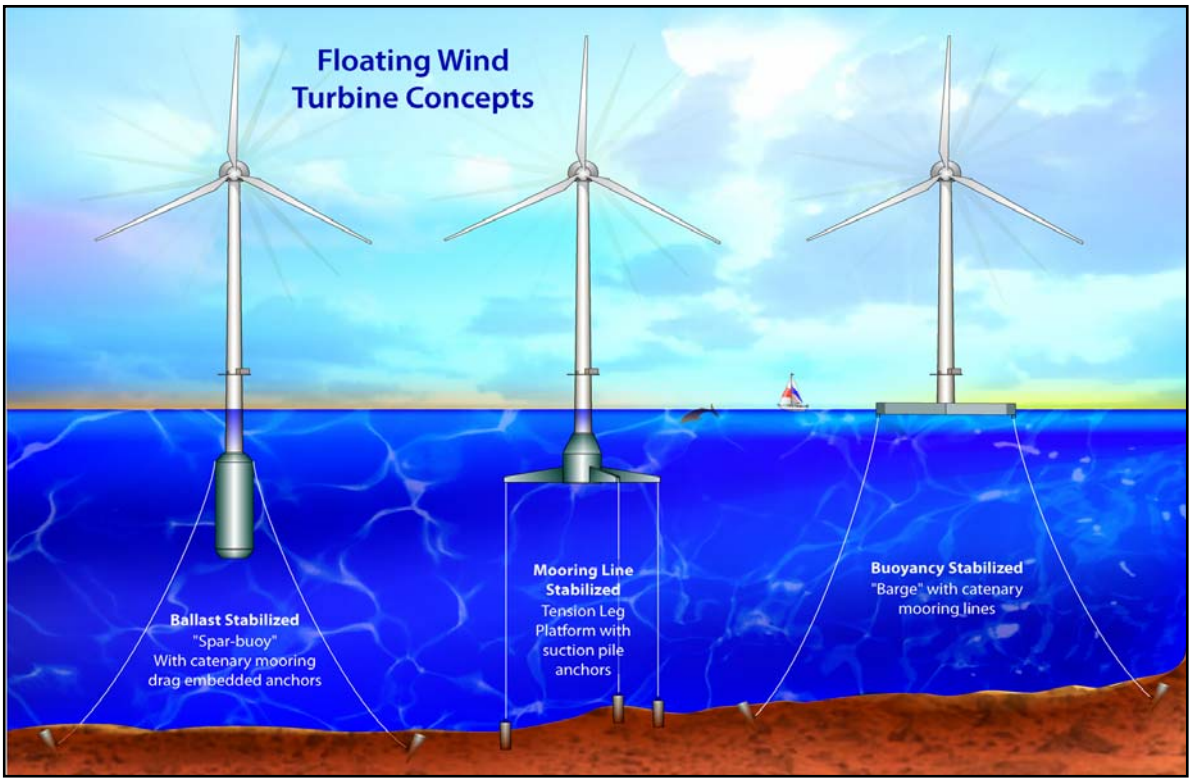

Figure 1. Floating wind turbine concepts.

Instabilities, or even marginal stabilities, can lead to rapid destructive failure or limit-cycle oscillations. Loads associated with limit-cycle oscillations usually result in ultimate-load or fatigue failure. The challenge for both onshore and offshore turbines is to devise design and control strategies that will eliminate instabilities while offering loads, performance, and cost benefits. This requires attention in several areas: accurate aero-servo-hydro-elastic modeling, developing stability analysis tools, detailed stability analyses, understanding adverse interactions causing instabilities, devising design and control strategies to decouple such interactions with minimal effect on loads and performance, and providing guidelines for avoiding instabilities. This paper presents progress in a narrow area: linearized stability analysis of a concept offshore turbine, for which governing equations are periodic. Understanding the underlying mechanisms and more elaborate stability analyses will be addressed in the future papers.

The barge supports a 3-bladed large (5MW) conventional upwind turbine. We use a conventional design for two reasons: (a) this is our first attempt at the hydro-aeroelastic stability analysis of a complete system, and (b) we do not yet have tools to model complexities associated with advanced

features. It should, however, be emphasized that the stability analysis techniques we present are equally applicable to unconventional designs that use advanced features.

The following section introduces the concept of instability and classifies instabilities. Next, we describe the stability analysis approach, which comprises state-space realization, multi-blade-coordinate transformation, and eigenanalysis. The subsequent section describes the 5MW turbine used in our study. Finally, we present results for two configurations: the onshore configuration (tower-base fixed to the ground) and the offshore configuration (tower base connected to a floating platform). Each configuration is analyzed under normal operating conditions and under parked (idling) conditions.

2. Discussion of Instabilities

2.1. Concept of instability.

Instability is a growing motion with two distinguishing features: a) it is *self-excited* and b) it grows *exponentially*. Self-excitation implies there is no explicit applied excitation. The self-excitation is induced by the motion itself. To understand this, consider a single-degree-of-freedom system:

$$m\ddot{x} + c\dot{x} + kx = f$$

where *m*, *c*, and *k* are its mass, damping, and stiffness. Usually, *f* is *f(t)*, an explicit function of time representing applied excitation. Now, suppose *f* is a function of the system motion. For simplicity, let it be proportional to the system velocity, i.e. $f = b\dot{x}$. The governing equation then becomes

$$m\ddot{x} + (c - b)\dot{x} + kx = 0$$

If *b* is greater than *c*, the effective damping, *(c-b)*, becomes negative and the system response *x(t)* grows exponentially, implying instability.

The example above illustrates a single-degree-of-freedom instability and that rarely occurs (an example is the torsion stall flutter). Often, more degrees of freedom are involved. Consider a flexible blade undergoing an oscillatory flap motion, *w(t)*. The flap motion induces inertia forces and changes in the aerodynamic forces, both circulatory and non-circulatory. These motion-induced forces can cause twisting moment. The twisting moment at a blade section depends on these induced forces as well as the relative locations of the section center of mass and the aerodynamic center with respect to the shear center. The elastic twist caused by this twisting moment introduces a change in the aerodynamic angle of attack and hence, a change in the aerodynamic flap force *f*. The phasing between *f* and *w*, under certain operating conditions, may be such that the motion-induced force *f* performs work on the blade, thereby pumping energy from the wind into the blade. This continuous pumping of energy leads to growing oscillatory motion of the blade and eventually to structural failure. This is an example of pitch-flap flutter instability, involving aeroelastic interactions between pitch and flap degrees of freedom. Energy-transfer mechanisms underlying other instabilities, in general, are different, are more complex, and may involve several degrees of freedom. However, all instabilities grow exponentially for linear systems. For a nonlinear system, the motion grows exponentially initially but may eventually settle down to limit-cycle high-amplitude oscillations. Figure 9b, which actually belongs to Section 5, illustrates this. Initially, when oscillations are small and the system behaves linearly, all responses grow exponentially. As oscillations grow, nonlinearities become significant, and limit-cycle oscillations set in.

In summary, instability leads to one of the following:

- Destructive failure.
- Limit-cycle oscillations causing excessive vibrations and fatigue.

Resonance should not be confused with instability. Resonant motion requires *external excitation* and grows *linearly* (not exponentially as in the case of instability). Also, in a resonance, the frequency of the external excitation coincides with one of the system's natural frequencies. Another distinction between resonance and instability is that while resonance occurs at *discrete-value* frequencies, instability occurs over distinct *ranges* of design or operating conditions.

2.2. Classification of instabilities.

Instabilities can be classified as static or dynamic. Static instabilities grow monotonically and do not involve inertia forces; examples are static divergence and aileron reversal for a wing. Most of the instabilities a wind turbine might encounter are likely to be dynamic and involving divergent oscillatory motions. Instabilities may also be classified according to the participating forces. Examples are aeroelastic instabilities, which involve participation of aerodynamic and elastic forces (e.g. pitch-flap and stall flutter), and hydro-aeroelastic instabilities, which involve participation of hydrodynamic and aeroelastic forces (e.g. platform-tower whirl of an offshore turbine). For a wind turbine, other classifications may be obtained by appropriately combining one or more of the following forces: mechanical, elastic, aerodynamic, hydrodynamic, control, and electrical. The source of self-excitation provides another way to classify instabilities:

Modes-coupled instabilities. These instabilities need two or more modes. Forces associated with one set of modes (modal set 1) pumps energy into another set of modes (modal set 2); the underlying reason is the phase difference between the two sets of modes. The increased motion of the second set amplifies forces in the first set, thereby setting up a destabilizing cycle. Examples are pitch-flap flutter and platform-tower whirl instabilities.

Nonlinear instabilities. Nonlinear phenomena such as dynamic stall, fluid sloshing, mechanical hysteresis, and von Karman vortices provide the source of self-excitation. A single mode usually suffices. Examples are stall flutter, mechanical chattering, and the infamous Strouhal instability observed on the Tacoma Narrows Bridge. Of all nonlinear instabilities, stall flutter is perhaps the most relevant to wind turbines.

Parametric instabilities. These instabilities are caused by parametric excitations brought on by time variation of the system parameters. Examples of these instabilities abound, ranging from a child on a swing forcing the swing higher by periodically raising and lowering his center of gravity to interacting galaxies ejecting galactic material. For a wind turbine, possibility of parametric instability is unlikely but not impossible. A periodic-control system in conjunction with periodic interaction of tower and rotor can cause such instability.

This paper focuses only on the mode-coupled class of instabilities because the likelihood of their occurrence is far greater than those of the other classes. Also, they are comparatively easier to analyze and require only linearized system models. We will model and analyze other instabilities in the future when we encounter novel designs and controls.

2.3. Eliminating instabilities.

Possible ways to eliminate instabilities include:

- Adding damping. This only works for marginal instabilities and only on certain types. For other types of instabilities, dampers can be ineffective or expensive and difficult to maintain.
- Alter design. For mode-coupled instabilities, this would imply altering design parameters so as to decouple the interacting modes.
- Introduce controls. This is the best method if the first two approaches are infeasible or expensive.
- Zoom-through operation. Some instabilities are so strong (usually called explosive instabilities) that none of the above methods would be cost-effective. An example is the Coleman instability involving coalescence of in-plane motion of rotor blades with rotor-shaft whirl. Luckily, for wind turbines, this instability occurs at rotor speeds much higher than the rotor nominal speed. Otherwise, the only way to mitigate instability would be to quickly rev the rotor through the coalescence range (helicopters do this routinely).

3. Stability Analysis Approach

The ultimate goals of stability analyses may be summarized as follows:

- Predict instabilities and near-instabilities (i.e., modes with small stability margins). Generating stability boundaries.
- Quantify stability margins and their sensitivity to design parameters and operating conditions.
- Identify underlying sources of self-excitation.
- Find the best ways to eliminate sources of self-excitation, e.g. modal decoupling.

Before these goals can be realized, however, we must perform stability analyses using the appropriate tools. The wide variety of stability analyses fall into two broad categories: a) the response-based approach, and b) the direct eigenanalysis approach. In the first approach, the system is excited with a set of well-defined forcing functions, and its stability features are extracted from either the response alone or from the response-input relation. This approach is useful if the instability is dominated by a nonlinear mechanism, e.g., stall flutter. However, this approach can be very time-intensive, and only the first few modes can be reliably captured. The second approach, direct eigenanalysis, is useful when the instability is governed by small excursions of the system motion about a specified operating point (or trajectory in the case of a time-varying system) and modal interactions dominate the instability. This approach is usually fast and accurate and captures all the participant modes. Below we summarize the four steps involved in this stability analysis approach and the tools used.

a. *State-Space Modeling*. We first develop a nonlinear model, which is either aeroelastic (for the onshore turbine) or hydro-aeroelastic (for the offshore turbine). The model is then linearized about steady-state operating conditions and transformed to a state-space model. The linearization and space-state modelling is discussed in References 28-30. We use FAST [30] coupled to AeroDyn [31,32], to first obtain the nonlinear aeroelastic or hydro-aeroelastic model and then extract the linearized state-space model. FAST, however, ignores the unsteady aerodynamic effects during linearization, though it accounts for them during formulation of its nonlinear equations. Unsteady-aerodynamic linearization, described in References 33-34 and 28, can be important for predicting certain instabilities and we plan to implement it in the near future. The states associated with the state-space model comprise n positions and n velocities, where n is the system degrees of freedom.

b. *Multi-Blade Coordinate Transformation.* The state-space model for a wind turbine system is in general periodic, i.e. some expressions in the model show periodic terms (where the period equals the time required for one rotor revolution). This periodicity arises because the dynamic interactions between the rotor and the tower-nacelle subsystem vary periodically as the rotor blades spin. Gravity, wind shear, and blade rotor controls also contribute periodic terms.

   Because of these periodic terms, a direct eigenanalysis on the state-space matrix may yield physically meaningless results. Researchers usually average the state-space matrices computed at different rotor azimuths. However, this can also lead to erroneous results; averaging eliminates all periodic terms and their contribution to system dynamics. To properly capture the effect of periodic terms, we perform a multi-blade coordinate transformation (MBC), which is also called Fourier Coordinate Transformation or Coleman Transformation in literature. MBC has been widely used in the helicopter field [35,36]. Reference 13 provides its theory basis and Reference 28 provides its implementation details. Realizing its importance, researchers have started applying it to wind turbines also [26,37-40].

   Note that the tower-nacelle subsystem feels the cumulative effect of all rotor blades. The dynamics of each individual blade not only varies azimuthally, but also differs from other blades at any given rotor azimuth. MBC helps capture the cumulative dynamics of all blades and transform it to a fixed reference frame associated with the tower tower-nacelle subsystem. Building on the basic theory explained in Ref 13, we developed an MBC tool that is quite powerful. It is applicable to any number of states, with arbitrary partitioning between fixed- and rotating-frame states. In addition to transforming the state-space matrices (a capability we use in the current paper), this

tool can also transform control, output, disturbance, mass, stiffness, and damping matrices (capability that we will use in future).

c. *Eigenanalysis*. Eigenanalysis generates eigenvalues and eigenvectors. The imaginary parts of the eigenvalues provide the frequencies of different modes and the real parts provide the associated modal dampings. The eigenvectors contain information on coupled modes, essential to identifying stability modes and underlying instability mechanisms.

   MBC, described earlier, also well-conditions the state-space matrix; it filters out all nonessential periodic terms (e.g. those associated with user-selected coordinates) and retains those that are inherent to the system. The MBC-transformed state-space matrix, though well-conditioned, is still periodic and strictly needs a Floquet-based eigenanalysis. However, this requires considerable effort, especially in the interpretation of eigenvalues and eigenvectors. If the system is weakly periodic, we may azimuth-average the MBC-transformed state matrices and obtain reasonably good results. This is the approach we use in the current paper. Note that azimuth-averaging must follow MBC; otherwise the results would be erroneous.

d. *Modal Interpretation.* As mentioned earlier, eigenvalues provide system frequencies and corresponding dampings. A positive real part of any eigenvalue implies negative damping or instability. To examine what causes a particular instability, we look at the corresponding eigenvector, usually complex, which shows how the various system states or modes couple in a particular instability. Interpretation of complex modes is an important step in the stability analysis approach and we used it extensively to obtain our results. However, it requires elaborate discussion, and we plan to address it in a separate paper. Suffice to say that modal interpretations are usually the most time- and effort-intensive part of stability analysis, requiring plots of complex eigenvectors and interpretation of magnitudes and phasing of the participating modes.

4. Description of the Wind Turbine

The conceptual wind turbine analyzed in this paper consists of two major parts: the above platform part and the floating platform part. The above-platform part resembles a conventional upwind, three-bladed wind turbine except that its rating is 5 MW, which is rather large for current onshore turbines. However, it is believed to be the minimum rating necessary to make a floating wind turbine system economical assuming the large proportion of costs are in the support platform [41]. The floating platform part uses the ITI Energy's barge concept, including mooring lines and moon pools [42]. A moon pool is a vertical well in the barge; the opening of the well extends right through the bottom of the barge. The ITI Energy concept envisages installing devices that would extract wave energy from the OWC (oscillating water column) within these moon pools. However, we do not model the effect these energy-extraction devices would have on system dynamics, for example the platform hydrodynamic damping.

4.1. *National Renewable Energy Laboratory (NREL) Baseline 5MW Wind Turbine.*

The conceptual above-platform part of the wind turbine analyzed in this paper consists of an upwind, three-bladed, 126-meter diameter rotor mounted upwind on top of an 87.6-meter tower. Jonkman et al [43] established this concept so as to best match a few existing 5-MW designs. Salient turbine properties are summarized in Table 1; other properties can be found in the cited reference. The NREL offshore 5-MW baseline wind turbine has been used to establish the reference specifications for a number of research projects supported by the U.S. Department of Energy's Wind Energy Technologies Program. In addition, the integrated European Union UpWind research program and the International Energy Agency Wind Annex XXIII Offshore Code Comparison Collaborative have adopted the NREL offshore 5-MW baseline wind turbine as their reference model.

4.2. *ITI Energy's Barge Platform.*
For offshore stability analysis, we mount the 5MW turbine, described in the earlier subsection, on top of a floating barge. We use a preliminary barge design developed by the Department of Naval Architecture and Marine Engineering at the Universities of Glasgow and Strathclyde under a contract with ITI Energy. The barge concept was chosen by ITI Energy because of its simplicity in design, fabrication, and installation. Not only is the barge designed to support a 5-MW baseline wind turbine, it also provides for an OWC wave power device. The barge is square and the wave energy is extracted from a square moon pool located at the center of the barge and within the base of the wind turbine tower. The barge is ballasted with sea water. To prevent it from drifting, the platform is moored by a system of eight catenary lines, two of which emanate from each corner of the bottom of the barge, so that they are 45° apart at the corner. Table 2 provides some details of the barge and mooring system. The concept is documented in greater detail in Ref 42.

Table 1. Summary of baseline wind turbine properties.

Rating	5 MW
Rotor Orientation	Upwind
Control	Variable Speed, Collective Pitch
Drivetrain	High Speed, Multiple Stage Gearbox
Rotor Diameter	126 m
Hub Height	90 m
Cut-In, Rated, Cut-Out Wind Speed	3 m/s, 11.4 m/s, 25 m/s
Cut-In, Rated Rotor Speed	6.9 rpm, 12.1 rpm
Rated Tip Speed	80 m/s
Overhang, Shaft Tilt, Precone	5 m, 5°, 2.5°
Blade structural damping ratio	2.5%
Tower structural damping ratio	1.0%
Rotor Mass	110,000 kg
Nacelle Mass	240,000 kg
Tower Mass	347,460 kg
Overall Center of Mass	(−0.2 m, 0.0 m, 64.0 m)

Table 2. Summary of the ITI Energy barge properties.

Size (W×L×H)	40 m × 40 m × 10 m
Moon pool (W×L×H)	10 m × 10 m × 10 m
Draft, Freeboard	4 m, 6 m
Water Displacement	6,000 m^3
Mass, Including Ballast	5,452,000 kg
Center of Mass (CM) below SWL	0.282 m
Roll Inertia about CM	726,900,000 $kg \cdot m^2$
Pitch Inertia about CM	726,900,000 $kg \cdot m^2$
Yaw Inertia about CM	1,453,900,000 $kg \cdot m^2$
Anchor (Water) Depth	150 m
Separation Between Opposing Anchors	773.8 m
Unstretched Line Length	473.3 m
Neutral Line Length Resting on Seabed	250 m
Line Diameter	0.0809 m
Line Mass Density	130.4 kg/m
Line Extensional Stiffness	589,000,000 N

FAST cannot yet model the OWC wave power device. Instead, we modeled the hydrodynamics of the barge by assuming that the moon pool is covered by a fixed plate located just below the free surface.

5. Results

We performed stability analyses on two configurations: an onshore configuration and an offshore configuration. The onshore configuration is the 5MW, 3-bladed, upwind turbine described in Section 4.1 with the tower base fixed to the ground. The offshore configuration is the onshore turbine mounted atop the floating barge described in Section 4.2. For each configuration, we consider two sets of operating conditions: normal operating conditions and parked conditions. In the parked condition, the generator torque is assumed to be zero, implying that the rotor is free to idle. All results, with one exception noted later, are obtained using a structural damping ratio of 1.0% for the tower and 2.5% for the blades. The choice of 2.5% damping for the blades is explained in Section 5.3. Because the linearization scheme in FAST cannot yet handle active controls, dynamic stall, or hydrodynamic radiation damping, we ignore these effects during all stability analyses.

5.1. *Onshore Configuration: Normal Operation.*

In the normal turbine operation, the wind speed can vary from 3 m/s (cut-in speed) to 25 m/s (cut-out speed). At a given wind speed, the rotor controller sets each blade's pitch and rotor speed to values depicted in Figure 2. These values ensure optimum performance in region 2 and power regulation in region 3 [43]. Stability analysis is performed using the approach described in Section 3. However, during stability analysis at each wind speed, the controller is disabled, i.e. the blade pitch angles and the rotor speed are kept fixed. The last step in the stability analysis, i.e. the eigenanalysis, provides eigenvalues and eigenvectors. The imaginary parts of the eigenvalues yield damped frequencies and the real parts yield modal dampings. Figures 3-5 show the stability results.

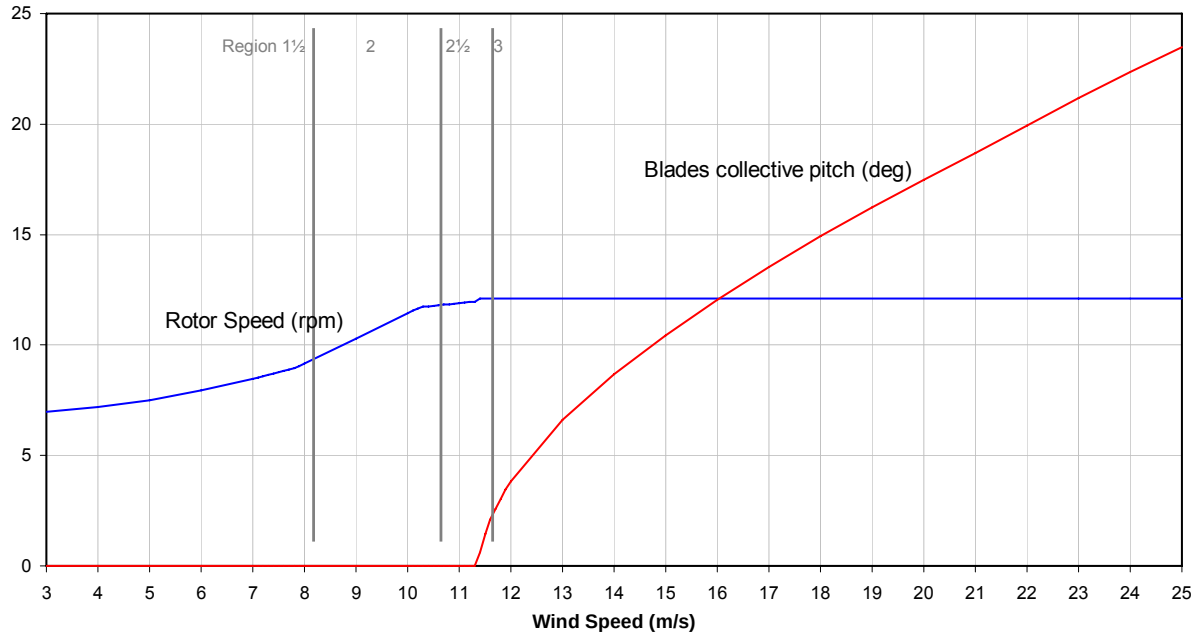

Figure 2. Variations of controlled blade-pitch angle and rotor speed with wind speed.

A consequence of the MBC transformation, described in Section 3, is that the individual *blade* modes are transformed to *rotor* modes. Consider the 1st lag (edgewise) mode of each blade. Instead of seeing three 1st lag modes, one for each blade, we see three rotor modes: Lag 1_coll, Lag 1_prog, and Lag 1_reg. These modes are respectively the first-lag collective, progressive, and regressive modes and are physically more meaningful. Note that the tower-nacelle-drivetrain system sees the cumulative effect of all the blades and not the individual blades. In fact, the rotor modes represent the cumulative effect of all the blades. The collective lag mode is a rotor mode in which all the blades bend, within

the rotor plane, in unison (either clockwise or anti-clockwise) with the same magnitude and phase. One can visualize that this rotor mode would interact with the drivetrain torsion mode. In the other two lag modes, the blades oscillate within the plane of the rotor in such a way that the effective center of mass of the rotor whirls about the rotor shaft. In the progressive mode, the center of mass whirls in the *same* direction as the rotor spin direction, but at an angular speed *higher* than the rotor speed. In the regressive mode, the center of mass whirls in a direction *opposite* to that of the rotor spin and at an angular speed *lower* than the rotor speed. References 26 and 37 explain these modes in more detail. One can visualize that the mass imbalance associated with the rotor center-of-mass whirl can induce whirling of the rotor shaft bending mode and to some extent the tower bending mode. FAST, however, cannot yet model the shaft bending and, therefore, our results do not show any drivetrain whirl.

As with the lag modes, the rotor exhibits flap modes that represent the cumulative effect of all the blades. Each mode, however, has a different physical significance and interacts differently with the fixed (tower-nacelle) system. The collective flap mode is a rotor mode in which all the blades flap, out of the rotor plane, in unison and with the same magnitude. One can visualize that in this mode, the rotor cones back and forth and interacts with the tower fore-aft mode. In the progressive flap mode, the rotor disk wobbles in the *same* direction as the rotor spin direction and at an angular speed *higher* than the rotor speed. In the regressive flap mode, the rotor disk wobbles in a direction *opposite* to that of the rotor spin direction and at an angular speed *lower* than the rotor speed. References 13, 26, and37 explain these modes in more detail.

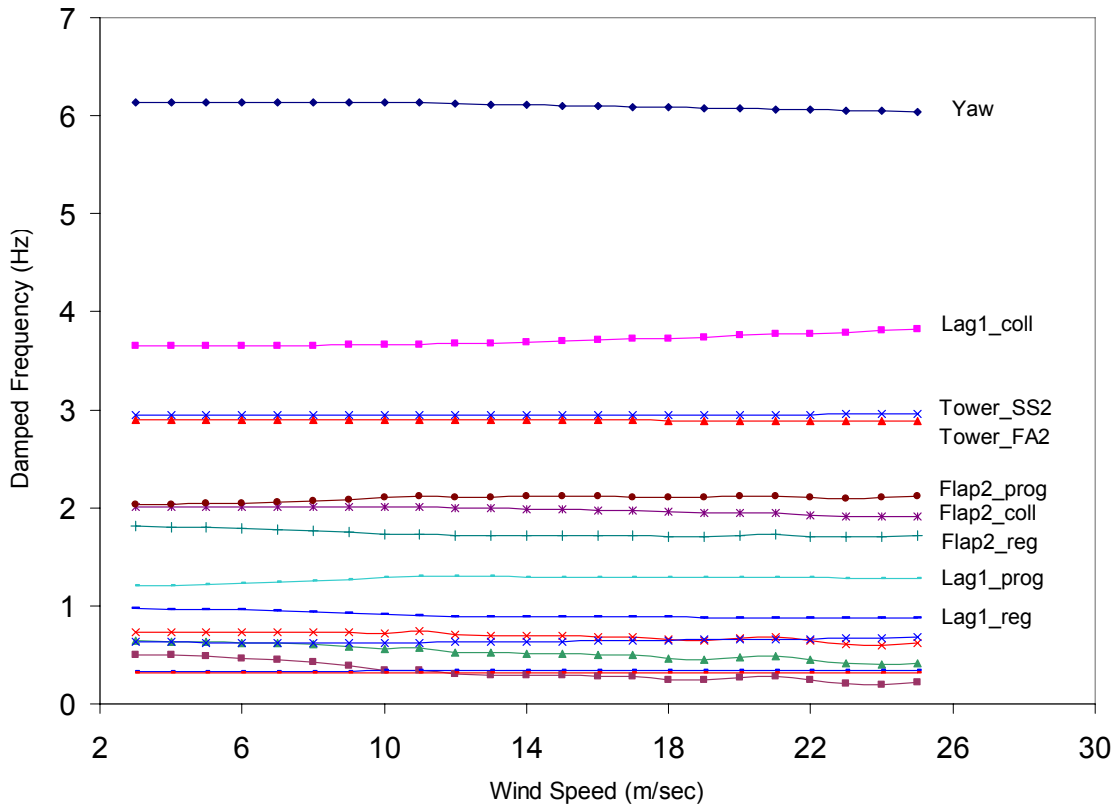

Figure 3. Variation of damped modal frequencies with wind speed (onshore configuration).

Figure 3 shows the variation of damped modal frequencies with wind speed. Note that the nacelle yaw frequency decreases somewhat with wind speed. This is because of the damping provided by the rotor-blades flapping motion, which couple with the yaw motion. We examined the eigenvector associated with the yaw mode to see this coupling. Eigenvectors are essential to identifying the stability modes and understanding the coupling of motions in each mode. Though we extensively used

eigenvectors to identify all stability modes presented in this paper, we cannot discuss them within the limited length of this paper.

To properly discern the variation of other frequencies, the results are re-plotted in Figure 4. Readers familiar with the isolated rotor modes, wherein the tower-nacelle subsystem is fully rigid, will notice interesting differences. For an isolated rotor spinning in a vacuum, progressive and regressive modal frequency curves are symmetric about the corresponding collective modal frequency curve; at any rotor speed, Ω, the progressive mode frequency is $\omega\_coll + \Omega$, and the regressive mode frequency is $\omega\_coll - \Omega$, where ω_coll is the collective mode frequency. However, this symmetry is lost for a full system because of two reasons. First, the different rotor modes interact differently with the tower-nacelle subsystem motion. Second, the aeroelastic interactions of the wind with the progressive, collective, and regressive modes can be drastically different. Note that the Lag1_coll frequency curve is not even located between the Lag1_prog and Lag1_reg curves, normally observed for an isolated rotor. This is because the 1st rotor lag collective mode strongly interacts with the torsionally-compliant drivetrain mode.

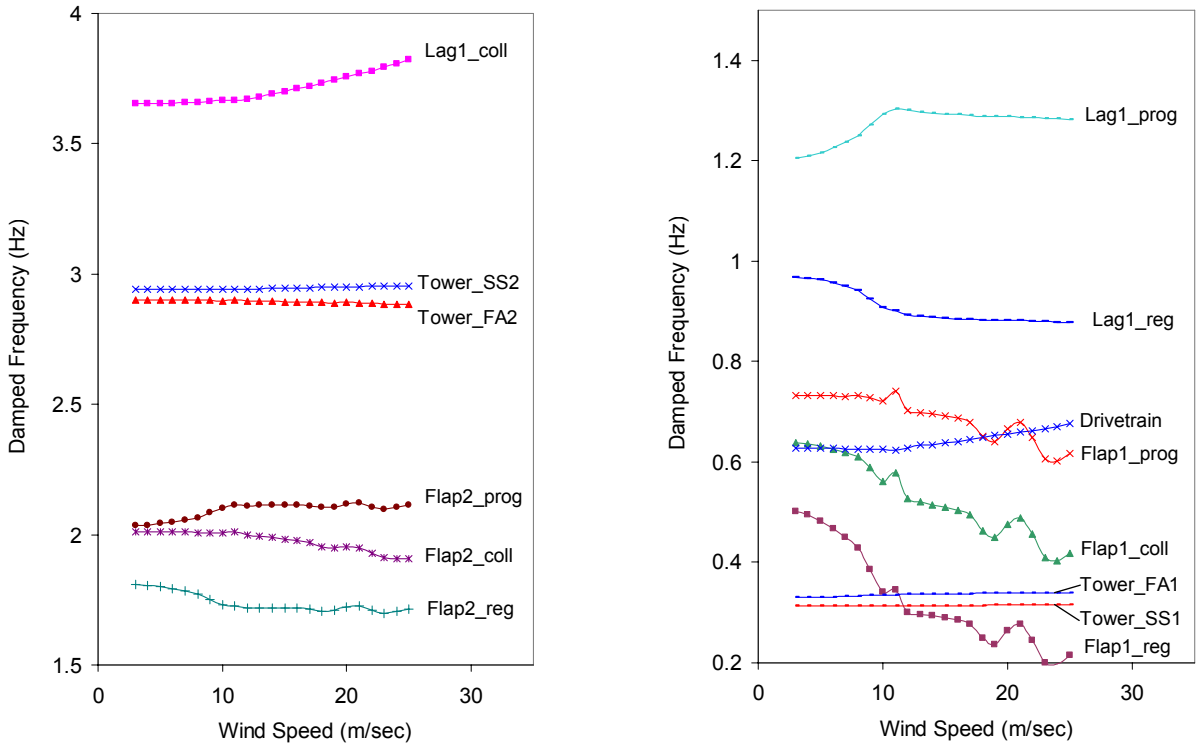

Figure 4. Variations of damped modal frequencies with wind speed (onshore configuration).

The exact physics behind the modal frequency trends, some of which show kinks near 11.3 m/s and 21 m/s wind speeds, is still under investigation. However, we make a few observations. Both the 1st rotor lag collective and the drivetrain modal frequencies increase beyond the 11.3 m/s wind speed. This cannot be a centrifugal stiffening effect because the rotor speed is held constant after this wind speed (see Figure 2). This is purely an aeroelastic effect brought in by changes in the wind speed and the blade pitch angle. Frequencies of the Flap2_coll, and Flap1_coll, and Flap1_prog modes decrease with wind speed, indicating a strong influence of aeroelastic couplings. A sudden change in the frequency trends near 11 m/s wind speed is due to the fact that the rotor speed is held constant beyond this wind speed (see Figure 2). Note that all tower modes are relatively insensitive to the wind speed.

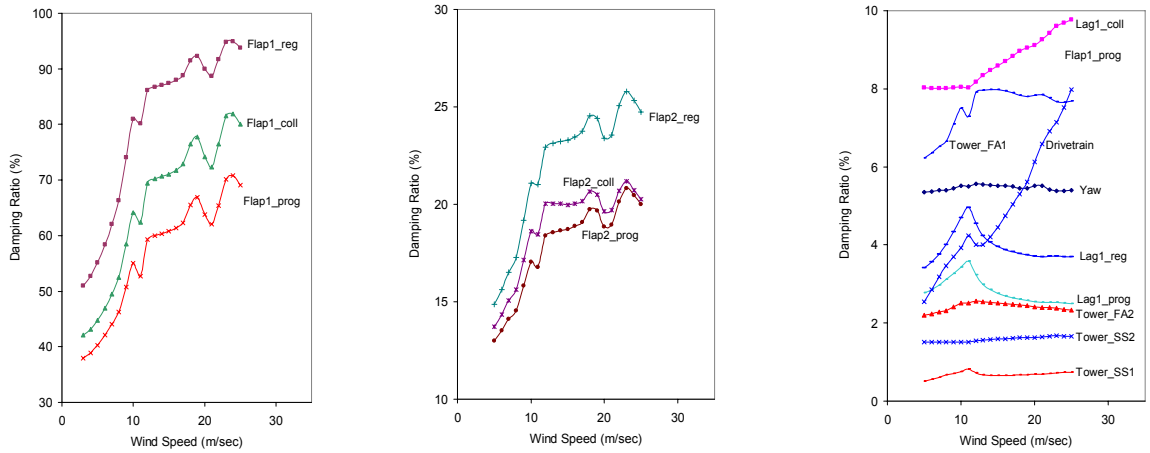

Figure 5. Variations of modal damping ratios with wind speed (onshore configuration).

Figure 5 shows the variation of modal damping ratios with wind speed. All modes have positive damping, implying that they are all stable. As expected, all flap modes are highly damped. However, damping of the rotor first flap modes exceeds 50% and is somewhat high; in our experience with typical rotors, this damping is usually in the 30%-50% range. This high damping suggests that the blade is quite light in comparison to its aerodynamic capability. Typical blades have a Lock number in the range 8-10 (a Lock number is a non-dimensional parameter that expresses the aerodynamic lift capability of a blade in comparison to its weight). The blade in this study has an effective Lock number of about 12. Damping of both the progressive and regressive lag modes increases rapidly as wind speed is increased from 3 m/s to about 11 m/s; thereafter it decreases and becomes almost constant beyond the wind speed of 22 m/s. The drivetrain frequency increases monotonically except near a wind speed of 12 m/s where it shows a slight dip. The tower 1st side-to-side mode is the least damped, with a maximum damping of about 0.8%. The tower 1st fore-aft mode is appreciably damped because of its coupling with the rotor collective flap modes, which we see are well-damped. The Lag1_reg and Lag1_prog modes show rapid increase in damping as the wind speed increases to 11.3 m/s. After this wind speed, the damping decreases rapidly until the wind speed reaches about 20 m/s. The drivetrain damping increases from 3.5% at 3 m/s wind speed to about 8% at 25 m/s wind speed.

5.2. *Offshore Configuration: Normal Operation.*

As with the onshore configuration, the wind speed varies from 3 m/s (cut-in speed) to 25 m/s (cut-out speed). The blades collective pitch and rotor speed are set to values shown in Figure 2. Stability analysis results are presented in Figures 6 and 7.

Figure 6 shows the variation of damped modal frequencies with wind speed. All modal frequencies are very similar to those obtained for the onshore configuration, except the tower 1st fore-aft and 1st side-to-side modes, which are appreciably affected by the presence of the platform. Whereas these frequencies were around 0.3 Hz for the onshore configuration, they are now around 0.55 Hz. The six lowest frequencies correspond to the six modes of the platform. Among these modes, the heave mode shows the highest frequency (around 0.13 Hz) and the sway/surge modes show the lowest frequency (around 0.008 Hz). The sway is defined as the side-to-side translation, and the surge is defined as the fore-aft translation of the barge. The platform modal frequencies depend on the barge buoyancy, mooring lines properties, and system inertia (this inertia includes the added hydrodynamic mass). Interestingly, all platform frequencies appear to be unaffected by the rotor speed. The platform yaw frequency decreases somewhat after the wind speed exceeds the 11.3 m/s value, though. (Recall that the rotor speed does not change after this wind speed). As for the platform mode shapes (not shown), they change somewhat with rotor speed because of the gyroscopic effect of the rotor.

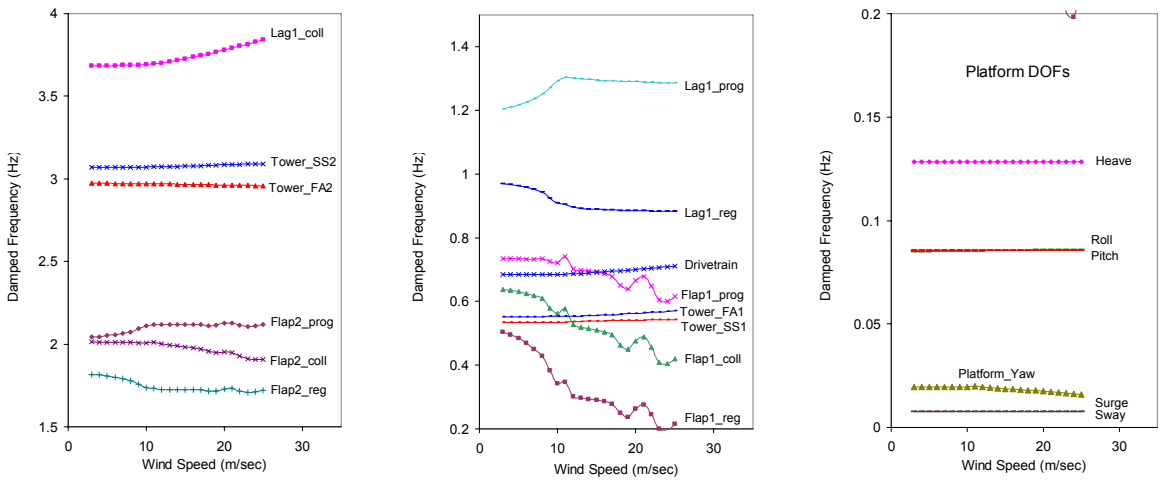

Figure 6. Variation of modal damped frequencies with wind speed (offshore configuration).

Figure 7 shows the variation of modal damping ratios with wind speed. The damping of the rotor modes is barely affected by the presence of the platform. The tower 1st fore-aft and side-to-side modal dampings are, however, significantly influenced through dynamic interactions with the platform. The tower side-to-side modal damping, though still the smallest as with the onshore configuration, now always stays above 1%; in fact, it reaches around 2.8% at 11.3m/ wind speed. On the other hand, the 1st tower fore-aft modal damping, which was between 6% to 8% for the onshore configuration, is now reduced and stays in the 2.8% to 5.5% range. Interestingly, the 1st tower fore-aft mode attains its minimal damping (2.8%) at 11.3 m/s wind speed, a speed at which the 1st fore-aft and side-to-side damping attains its maximum value. Even though the tower first side-to-side and fore-aft modes are still stable, reduced damping can translate into higher tower vibrations.

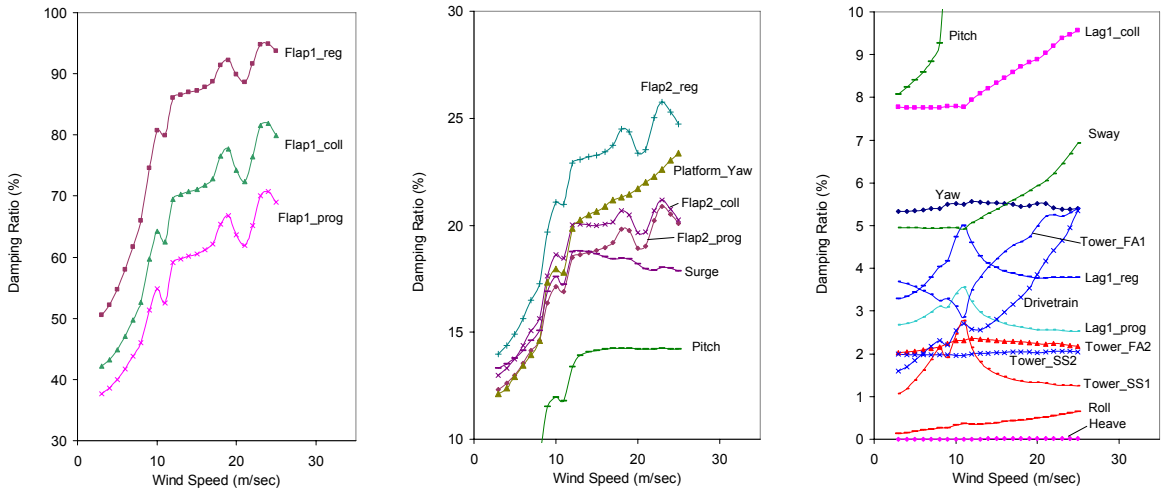

Figure 7. Variation of modal damping ratios with wind speed (offshore configuration).

All the platform modes are stable. The roll and heave modes, however, show marginal damping ratios and are, therefore, susceptible to higher vibration levels. Among the platform modes, the platform yaw, surge and the pitch modes show the highest damping, presumably because of their strong coupling with the rotor flap modes, which are highly damped. All the platform modal dampings increase with wind speed, except the pitch and sway modal dampings, which stay almost constant once the wind speed exceeds 14 m/s. Note in particular the appreciable damping of the platform yaw

mode; it stays in the range 12-23% under normal operating conditions. We will see later (Section 5.4) that this mode can become unstable under certain idling conditions.

5.3. *Onshore Configuration: Parked (idle) Condition*.
Now we consider a few parked turbine conditions mandated by the International Electrotechnical Commission (IEC) design standard [44,45]. For these conditions, loads analysis [41] suggested that the turbine might be encountering instabilities under parked conditions. To support the loads analysis, we performed a systematic stability analysis starting with some exploratory studies. A useful result from the exploratory studies is shown in Figure 8. The turbine is idling in a 50 m/s wind and the nacelle yaw is set at 30^0 with respect to the wind direction.

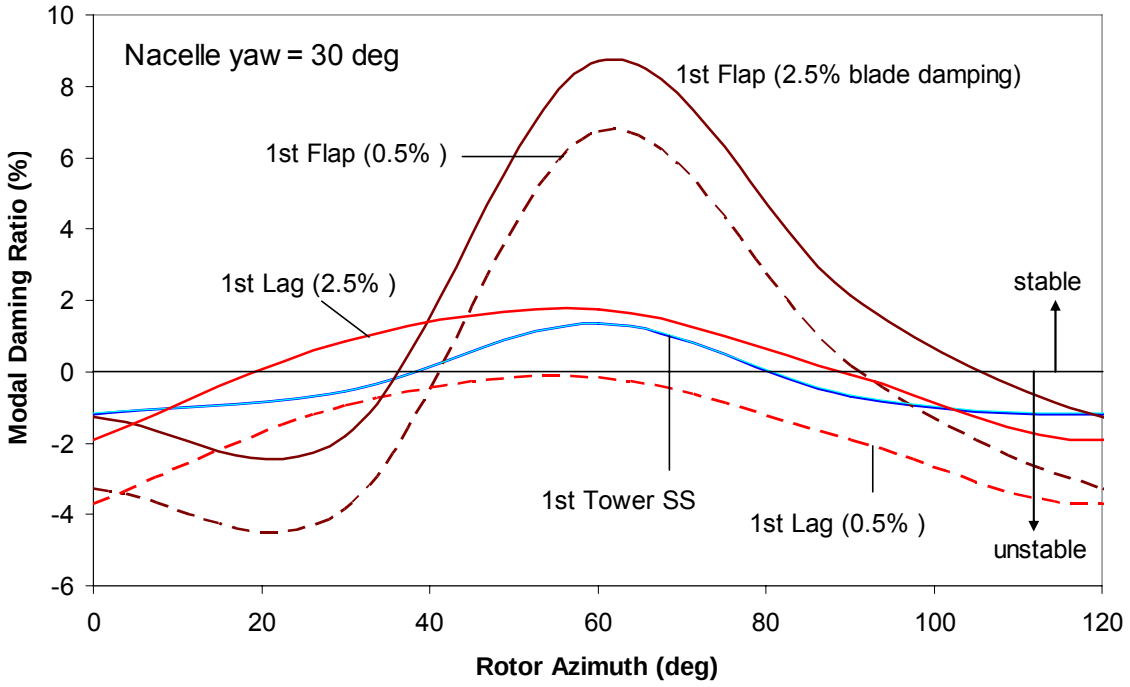

Figure 8. Variation of modal damping ratios with rotor azimuth (parked onshore turbine).

The figure shows the three least-damped modes when the turbine is parked. Though the modes are labeled as 1st flap, 1st lag, and 1st tower side-to-side modes, all show significant coupling with other turbine modes. These labels only identify the dominant participating motion in a particular mode. Because the rotor is not spinning, MBC is not applicable and the results are obtained using a direct eigenanalysis. The rotor azimuth position refers to the azimuth of the reference blade (a zero azimuth implies that the reference blade is pointed up). Results are obtained using two values of the blade structural damping: a 0.5% structural damping, which is typical of metallic blades, and a 2.5% structural damping, which represents the higher side of the range of damping values for composite blades. Each blade is assumed feathered at 90^0 when the turbine is parked. These results are obtained with nacelle yaw set at 30^0.

First note that, irrespective of the structural damping used, all shown modes exhibit negative damping when the rotor azimuth is in the $0\text{-}20^0$ range, implying that the three modes are unstable over this azimuth range. Understandably, this range would be different if a nacelle yaw position other than 30^0 is used. Second, note that higher blade structural damping, though helpful for the blade modes, does not affect the stability of the tower mode. Third, note that the three modal dampings are very sensitive to rotor azimuth position. Though a systematic study of the underlying cause of these

instabilities is yet to be performed, a preliminary investigation suggests that these might be stall-induced.

While Figure 8 shows that instabilities are sensitive to the rotor azimuth, it also raises a question: which azimuth position would the rotor assume when the turbine is parked and free to idle? The answer is that it depends on the wind speed, the nacelle yaw, and the pitch angles to which the blades are set during idling. The IEC standards for the parked turbine condition provide guidance on how the wind speeds and the nacelle yaw angles should be selected (see Table 3). The blade pitch settings shown in the Table conform to the standard active-pitch-to-feather practice most turbines follow when the rotor is idling.

Table 3. Design load cases for the parked (idling) turbine.

DLC	Wind Model	Wind Speed	Controls/Event	Specific value used in the current study
6.1a		$V_{hub} = V_{50}$	Yaw=0^0, $\pm 8^0$; all blades feathered at 90^0	V_{50} = 50 m/s
6.2a	EWM	$V_{hub} = V_{50}$	Loss of grid → -180^0 < yaw < 180^0 all blades feathered at 90^0	V_{50} = 50 m/s
6.3a	EWM	$V_{hub} = V_1$	Yaw=0^0, $\pm 20^0$; all blades feathered at 90^0	V_1 = 40 m/s
7.1a	EWM	$V_{hub} = V_1$	Yaw=0^0, $\pm 8^0$; one blade seized at 0^0 Other blades feathered at 90^0	V_1 = 40 m/s

We first present stability results for the design load cases (DLCs) 6.1a and 6.2a. For these cases, as Table 3 shows, the wind speed is 50 m/s and all blades are set at 90^0. The nacelle yaw angle is varied.

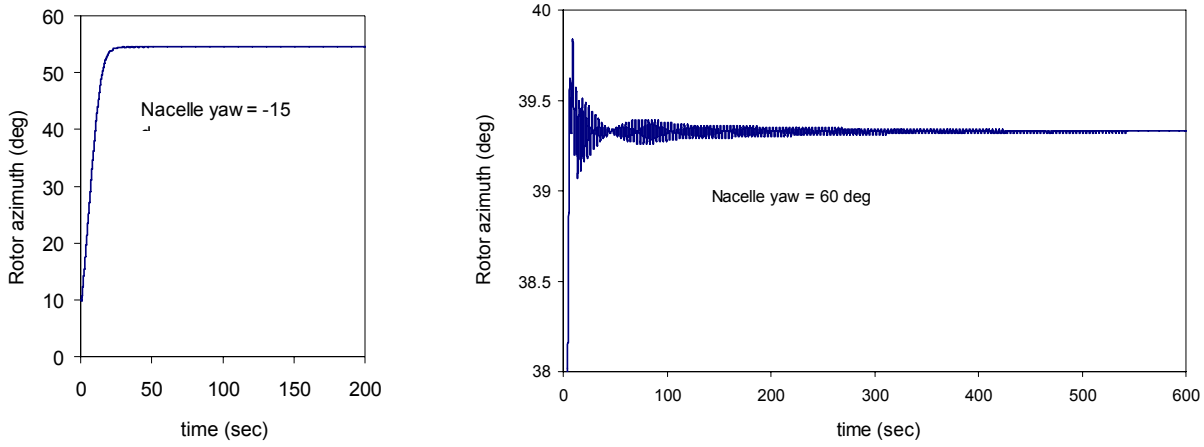

Figure 9a. Variation of the rotor azimuth with time (parked onshore turbine).

Depending on the nacelle yaw setting, the idling rotor would respond in one of the following ways: it can settle to a specific azimuth position with or without oscillations (Figure 9a), it can settle to an oscillatory back-and-forth rotor angular motion about a mean azimuth position (Figure 9b), or it can spin continuously at a very low rpm (no figure). If the rotor assumes a mean azimuth position, we linearize the system model about that yaw position and perform a direct eigenanalysis to obtain stability modes. If the rotor spins slowly at some rpm, we perform MBC followed by eigenanalysis. The stability results are summarized in Table 4. The unstable modes are shown in red. Note that flap mode is stable for all cases. Both the 1st tower and 1st lag modes exhibit instabilities when the nacelle yaw is either -30^0 or 20^0. When nacelle yaw is 30^0, only the 1st lag model shows instability. Only marginal instabilities are observed for other design load cases (6.3a and 7.1a) and the results are not presented.

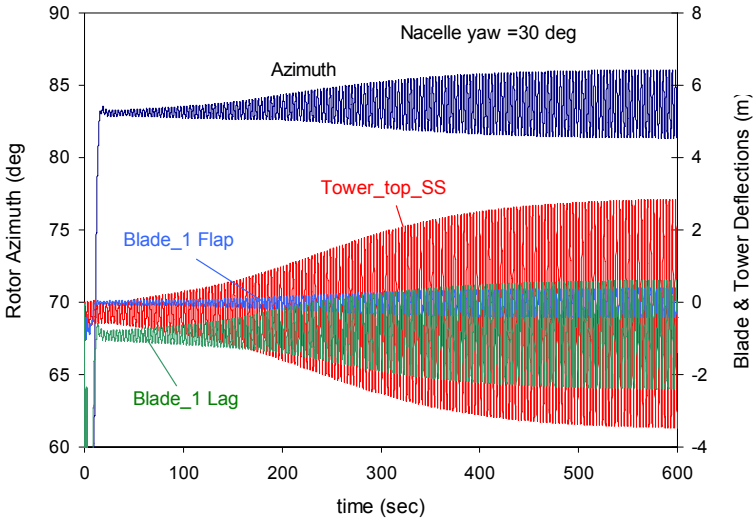

Figure 9b. Variation of the rotor azimuth with time (parked onshore turbine).

Table 4. Modal damping ratios (%) for different nacelle-yaw settings (DLCs 6.1a & 6.2a)

Nacelle Yaw (deg)	1st Tower Side-Side	1st Flap	1st Lag
-60	0.21628	1.6064	3.2695
-45	0.64873	2.5098	2.5884
-30	0.27054	2.0333	-0.26399
-20	-0.58981	2.1163	-0.038306
-15	0.97208	2.7269	3.2742
-8	0.80674	3.0489	3.4447
0	0.76662	3.9751	2.8624
8	0.84679	3.0435	3.1454
15	0.91099	2.5815	3.1753
20	0.47636	2.0345	-2.146
30	-0.66231	2.1703	-0.083306
45	0.67591	2.7246	2.2767
60	0.38493	2.3133	2.3654

5.4. *Offshore Configuration: Parked (idle) Condition.*

For the offshore parked turbine, we again consider the same design load cases as for the onshore configuration and also follow the same stability analysis approach. Design load case 7.1a exhibits the most severe instabilities and results for the three least damped modes are shown in Table 5. Unstable cases are identified in red.

The tower 1st side-to-side mode is marginally stable and the platform roll mode is unstable when the nacelle yaw is zero. However, the platform yaw mode exhibits strong instability at all yaw angles. It should be emphasized, however, that viscous effects on the mooring lines and yaw motion have been ignored. Also, the effect of oscillating water columns (OWCs) in the barge moon pools has been neglected. Because the OWCs are designed to extract energy, we believe the barge pitch and roll dampings, which are already positive, will increase substantially. For stabilization of the yaw mode, we have several options, e.g. attaching damping plates to the bottom of the barge and using crowfeet to attach the mooring lines to the barge.

Table 5. Modal damping ratios (%) for different nacelle-yaw settings (DLCs 7.1a)

Nacelle Yaw (deg)	1st Tower Side-Side	Platform Roll	Platform Yaw
-8	3.842	3.4911	-21.98
0	0. 81831	-4.3394	-14.047
8	2.1976	2.0333	-3.6788

6. Conclusions and Future Work

Both onshore and offshore configurations are stable under normal operating conditions. However, under certain parked (idling) conditions, both turbine and platform modes, in particular the yaw mode, show instabilities. These instabilities are sensitive to rotor azimuth and nacelle yaw positions. The rotor blades appear to have a high Lock number, which leads to high flap dampings. While beneficial to flap motion, higher Lock numbers can also render instabilities more severe.

To mitigate instabilities under idling conditions, we tried several strategies, e.g. feathering the blades at non-90^0 angles (to get low rotor speeds) and applying generator brake. Though results are not presented, both strategies showed an overall improvement of stability. However, for the slow-turning rotor case, instabilities were aggravated for certain nacelle yaw settings. Results were also mixed for the braked; certain combination of rotor azimuth and nacelle yaw positions aggravated the instabilities. We plan to further explore both these strategies in addition to reducing the blade Lock number. Next, we plan to include the unsteady aerodynamic effects in our linearized models. We also plan to integrate FAST with models of the OWCs to get more stability results. Other future tasks include: understanding instability mechanisms (modal couplings in particular), trying alternate designs and controls to improve stability, introducing Floquet analysis to handle periodicity, and providing design guidelines for avoiding instabilities.

Acknowledgments

Thanks are due to Ian Edwards of ITI Energy for sponsoring the loads & stability analysis project and Dr. Nigel Barltrop and Willem Vijhuizen of the Universities of Glasgow and Strathclyde for designing the barge and mooring system concept. We also thank Walt Musial and Sandy Butterfield of NREL for leading the Offshore Wind Energy Program at NREL. We would also like to thank Marshall Buhl of NREL for some very useful suggestions. This work was performed in support of the U.S. Department of Energy under contract number DE-AC36-99-GO10337 and in support of a Cooperative Research and Development Agreement with ITI Energy, number CRD-06-178.

References

[1] Musial, W.; Butterfield, S.; and Ram, B.; "Energy From Offshore Wind," *2006 Offshore Technology Conference, 1-4 May 2006, Houston, TX* [CD-ROM], Richardson, TX: Offshore Technology Conference, May 2006, OTC 18355, NREL/CP-500-39450.

[2] Musial, Walt; Butterfield, Sandy; and Boone, Andrew, "Feasibility of Floating Platform Systems for Wind Turbines," *A Collection of the 2004 ASME Wind Energy Symposium Technical Papers Presented at the 42nd AIAA Aerospace Sciences Meeting and Exhibit, 5–7*

January 2004, Reno Nevada, USA, New York: American Institute of Aeronautics and Astronautics, Inc. (AIAA) and American Society of Mechanical Engineers (ASME), January 2004, pp. 476–486, NREL/CP-500-36504.

[3] Watson, Greg, et al, "A Framework for Offshore Wind Energy Development in the United States," *Massachusetts Technology Collaborative (MTC)* [online publication], URL: http://www.mtpc.org/offshore/final_09_20.pdf, [cited 17 November 2005].

[4] Musial, W. and Butterfield, S., "Future for Offshore Wind Energy in the United States," *EnergyOcean Proceedings, June 2004, Palm Beach Florida, USA*, NREL/CP-500-36313.

[5] Butterfield, Sandy; Musial, Walt; Jonkman, Jason; Sclavounos, Paul; and Wayman, Libby, "Engineering Challenges for Floating Offshore Wind Turbines," *Copenhagen Offshore Wind 2005 Conference and Expedition Proceedings, 26–28 October 2005, Copenhagen, Denmark* [CD-ROM], Copenhagen, Denmark: Danish Wind Energy Association, October 2005.

[6] Lee, Kwang Hyun, "Responses of Floating Wind Turbines to Wind and Wave Excitation," M.S. Dissertation, Department of Ocean Engineering, Massachusetts Institute of Technology, Cambridge, Massachusetts, USA, January 2005.

[7] Wayman, E. N.; Sclavounos, P. D.; Butterfield, S.; Jonkman, J.; and Musial, W.; "Coupled Dynamic Modeling of Floating Wind Turbine Systems," *2006 Offshore Technology Conference, 1-4 May 2006, Houston, TX* [CD-ROM], Richardson, TX: Offshore Technology Conference, May 2006, OTC 18287, NREL/CP-500-39481.

[8] Wayman, Elizabeth, "Coupled Dynamics and Economic Analysis of Floating Wind Turbine Systems," M.S. Dissertation, Department of Mechanical Engineering, Massachusetts Institute of Technology, Cambridge, Massachusetts, USA, June 2006.

[9] Henderson, Andrew R. and Patel, Minoo H., "On the Modelling of a Floating Offshore Wind Turbine," *Wind Energy*, Vol. 6, No. 1, February 2003, pp. 53–86.

[10] Withee, John E., "Fully Coupled Dynamic Analysis of a Floating Wind Turbine System," Ph.D. Dissertation, Department of Ocean Engineering, Massachusetts Institute of Technology, Cambridge, Massachusetts, USA, 2004.

[11] Jonkman, Jason M. and Sclavounos, Paul D., "Development of Fully Coupled Aeroelastic and Hydrodynamic Models for Offshore Wind Turbines," *44th AIAA Aerospace Sciences Meeting and Exhibit, 9-12 January 2006, Reno, NV, AIAA Meeting Papers on Disc* [CD-ROM], Reston, VA: American Institute of Aeronautics and Astronautics, January 2006, AIAA-2006-995, NREL/CP-500-39066.

[12] Jonkman, J. M. and Buhl, M. L., Jr., "Development and Verification of a Fully Coupled Simulator for Offshore Wind Turbines," *45th AIAA Aerospace Sciences Meeting and Exhibit, 8–11 January 2007, Reno, NV, AIAA Meeting Papers on Disc* [CD-ROM], Reston, VA: American Institute of Aeronautics and Astronautics, January 2007, AIAA-2007-212, NREL/CP-500-40979, Golden, CO: National Renewable Energy Laboratory.

[13] Johnson, W. *Helicopter Theory*. Princeton University Press, New Jersey, 1980.

[14] Fung, Y.C. *An Introduction to the Theory of Aeroelasticity*. John Wiley and Sons, Inc., 1955.

[15] Bisplinghoff, R.L., Ashley, H. and Halfman, R.L. Aeroelasticity. Dover Publications, 1955.

[16] Lobitz, D.W., "Aeroelastic stability predictions for a MW-sized blade," *Wind Energy*, 7:211–224, 2004.

[17] Lobitz, D.W., "Parameter sensitivities affecting the flutter speed of a MW-sized blade," *Journal of Solar Energy Engineering, Transactions of the ASME*, 127(4):538–543, 2005.

[18] Petersen, J. T., Madsen, H. Aa., Bj¨orck, A., Enevoldsen, P., Øye, S., Ganander, H. and Winkelaar, D., "Prediction of dynamic loads and induced vibrations in stall," Technical Report Risø-R-1045(EN), Risø National Laboratory, Denmark, May 1998.

[19] K. Thomsen, J. T. Petersen, E. Nim, S. Øye, and B. Petersen, "A method for determination of damping for edgewise blade vibrations," Wind Energy, 3:233–246, 2001.

[20] F. Rasmussen, J. T. Petersen, and H. Aa. Madsen, "Dynamic stall and aerodynamic damping," *ASME Journal of Solar Energy Engineering*, 121:150–155, 1999.

[21] P. K. Chaviaropoulos, "Flap/lead-lag aeroelastic stability of wind turbine blades," *Wind Energy*, 4:183–200, 2001.
[22] A. Bj¨orck, J. Dahlberg, A. ¨Ostman, and H. Ganander, "Computations of aerodynamic damping for blade vibrations in stall," the *1997 European Wind Energy Conference*, pages 503–507, Dublin Castle, Ireland, October 1997.
[23] Holierhoek, J.G.,"Investigation into the possibility of flap-lag-stall flutter," 45th AIAA Aerospace Sciences Meeting and Exhibit, Reno, Nevada, January 2007.
[24] C.W. Acree, Jr., R.J. Peyran, and W. Johnson, "Rotor Design for Whirln Flutter: An Examination of Options for Improving Tiltrotor Aeroelastic Stability Margins," presented at the American Helicopter Society 55th Annual Forum. Montreal, Quebec, Canada, May 1999.
[25] M.W. Nixon, "Parametric Studies for Tiltrotor Aeroelastic Stability in High Speed Flight," *Journal of the American Helicopter Society*, Vol. 38, No. 4, October 1993.
[26] Bir, G.S., Wright, A.D. and Butterfiled, S., "Stability Analysis of Variable-Speed Wind Turbines", Proceedings of the 1997 ASME Wind Energy Symposium, Reno, January 6-9, 1997.
[27] Bir, G.S. and Chopra, I., "Aeromechanical Instability of Rotorcraft with Advanced Geometry Blades," Journal of Mathematical and Computer Modeling, Vol. 19, N0. 3/4, pp. 159-191, 1994.
[28] Bir, G., Chopra, I., et al. "University of Maryland Advanced Rotor Code (UMARC) Theory Manual," Technical Report UM-AERO 94-18, Center for Rotorcraft Education and Research, University of Maryland, College Park, July 1994.
[29] K. Stol and G. Bir, "SymDyn User's Guide," NREL/EL-500-33845. Golden, Colorado, National Renewable Energy Laboratory.
[30] Jonkman, J. M. and Buhl, M. L., Jr., "FAST User's Guide," NREL/EL-500-29798, Golden, CO: National Renewable Energy Laboratory, October 2004.
[31] Laino, D. J. and Hansen, A. C., "User's Guide to the Computer Software Routines AeroDyn Interface for ADAMS®," Salt Lake City, UT: Windward Engineering LLC, Prepared for the National Renewable Energy Laboratory under Subcontract No. TCX-9-29209-01, September 2001.
[32] Moriarty, P. J. and Hansen, A. C., "AeroDyn Theory Manual," NREL/EL-500-36881, Golden, CO: National Renewable Energy Laboratory, December 2005.
[33] M. H. Hansen, M. Gaunaa, and H. Aa. Madsen. A Beddoes-Leishman type dynamic stall model in state-space and indicial formulations. Technical Report Risø–R–1354(EN), Risø National Laboratory, Denmark, 2004.
[34] Leishman, J.G. and Nguyen, K.Q., "State-Space Representattion of Unsteady Airfoil Behavior," *AIAA Jornal*, Vol. 28, N0. 5, pp. 836-844, May 1990.
[35] Coleman, R.P. and Feingold, A.M., "Theory of Self-Excited Mechanical Oscillations of Helicopter Rotors with Hinged Blades," NASA TN 3844, February 1957.
[36] Hohenemser, K.H. and Yin, S.K.,"Some Applications of the Method of Multi-Blade Coordinates," *Journal of American Helicopter Society*, 17(3), pp 3-12 (1972).
[37] M. H. Hansen, "Improved modal dynamics of wind turbines to avoid stall-induced vibrations," Wind Energy, 6:179-195, 2003.
[38] V. A. Riziotis, S. G. Voutsinas, E. S. Politis, and P. K. Chaviaropoulos. Aeroelastic stability of wind turbines: The problem, the methods and the issues. Wind Energy, 7(4):373–392, 2004.
[39] Hansen, M. H., "Stability analysis of three-bladed turbines using an eigenvalue approach," *2004 ASME Wind Energy Symposium*, pages 192–202, Reno, January 2004.
[40] Bir, G., "Understanding Whirl Modal Behavior of a Wind Turbine," proceedings of the 20th International Modal Analysis Conference, Los Angeles, California, February 4-7, 2002.
[41] Jonkman, J. M. and Buhl, M. L., Jr., "Loads Analysis of a Floating Offshore Wind Turbine Using Fully Coupled Simulation," to be presented at *the American Wind Energy Association, WINDPOWER 2007 Conference and Exhibition*, June 2007.

[42] Vijfhuizen, W. J. M. J, "Design of a Wind and Wave Power Barge," M.S. Dissertation, Department of Naval Architecture and Mechanical Engineering, Universities of Glasgow and Strathclyde, Glasgow, Scotland, September 2006.
[43] Jonkman, J.; Butterfield, S.; Musial, W.; and Scott, G., "Definition of a 5-MW Reference Wind Turbine for Offshore System Development," NREL/TP-500-38060, Golden, CO: National Renewable Energy Laboratory, February 2007 (to be published).
[44] IEC 61400–1 Ed. 3, *Wind Turbines – Part 1: Design Requirements*, International Electrotechnical Commission (IEC), 2005.
[45] IEC 61400–3, *Wind Turbines – Part 3: Design Requirements for Offshore Wind Turbines*, International Electrotechnical Commission (IEC), 2006 (to be published).